NASA/TP—2013–217487

Testing of an Annular Linear Induction Pump for the Fission Surface Power Technology Demonstration Unit

K.A. Polzin, J.B. Pearson, and K. Webster
Marshall Space Flight Center, Huntsville, Alabama

T.J. Godfroy
Maximum Technology Corporation, Huntsville, Alabama

J.A. Bossard
BSRD, LLC/Yetispace, Inc., Huntsville, Alabama

August 2013

The NASA STI Program…in Profile

Since its founding, NASA has been dedicated to the advancement of aeronautics and space science. The NASA Scientific and Technical Information (STI) Program Office plays a key part in helping NASA maintain this important role.

The NASA STI Program Office is operated by Langley Research Center, the lead center for NASA's scientific and technical information. The NASA STI Program Office provides access to the NASA STI Database, the largest collection of aeronautical and space science STI in the world. The Program Office is also NASA's institutional mechanism for disseminating the results of its research and development activities. These results are published by NASA in the NASA STI Report Series, which includes the following report types:

- TECHNICAL PUBLICATION. Reports of completed research or a major significant phase of research that present the results of NASA programs and include extensive data or theoretical analysis. Includes compilations of significant scientific and technical data and information deemed to be of continuing reference value. NASA's counterpart of peer-reviewed formal professional papers but has less stringent limitations on manuscript length and extent of graphic presentations.

- TECHNICAL MEMORANDUM. Scientific and technical findings that are preliminary or of specialized interest, e.g., quick release reports, working papers, and bibliographies that contain minimal annotation. Does not contain extensive analysis.

- CONTRACTOR REPORT. Scientific and technical findings by NASA-sponsored contractors and grantees.

- CONFERENCE PUBLICATION. Collected papers from scientific and technical conferences, symposia, seminars, or other meetings sponsored or cosponsored by NASA.

- SPECIAL PUBLICATION. Scientific, technical, or historical information from NASA programs, projects, and mission, often concerned with subjects having substantial public interest.

- TECHNICAL TRANSLATION. English-language translations of foreign scientific and technical material pertinent to NASA's mission.

Specialized services that complement the STI Program Office's diverse offerings include creating custom thesauri, building customized databases, organizing and publishing research results…even providing videos.

For more information about the NASA STI Program Office, see the following:

- Access the NASA STI program home page at <http://www.sti.nasa.gov>

- E-mail your question via the Internet to <help@sti.nasa.gov>

- Fax your question to the NASA STI Help Desk at 443–757–5803

- Phone the NASA STI Help Desk at 443–757–5802

- Write to:
  NASA STI Help Desk
  NASA Center for AeroSpace Information
  7115 Standard Drive
  Hanover, MD 21076–1320

Testing of an Annular Linear Induction Pump for the Fission Surface Power Technology Demonstration Unit

K.A. Polzin, J.B. Pearson, and K. Webster
Marshall Space Flight Center, Huntsville, Alabama

T.J. Godfroy
Maximum Technology Corporation, Huntsville, Alabama

J.A. Bossard
BSRD, LLC/Yetispace, Inc., Huntsville, Alabama

TRADEMARKS

Trade names and trademarks are used in this report for identification only. This usage does not constitute an official endorsement, either expressed or implied, by the National Aeronautics and Space Administration.

TABLE OF CONTENTS

LIST OF FIGURES

LIST OF TABLES

LIST OF ACRONYMS AND SYMBOLS

AC	alternating current
ALIP	annular linear induction pump
ATC	ALIP test circuit
DAQ	data acquisition
DC	direct current
EM	electromagnetic
FSP	fission surface power
GFSSP	Generalized Fluid System Simulation Program
He	helium
ID	inner diameter
INL	Idaho National Laboratory
MSFC	Marshall Space Flight Center
NaK	sodium potassium
RMS	root mean square
SS	stainless steel
TDU	technology demonstration unit
TP	Technical Publication
VFD	variable frequency drive
VFS	variable frequency power supply

NOMENCLATURE

A_{RMS}	line current in amperes (RMS)
C_p	specific heat
C_v	flow coefficient
D_0	ATC tube inside diameter
D_{equiv}	equivalent diameter
D_r	heater element diameter
l	physical immersion heater length
l_{equiv}	equivalent tube length
n	number of heater elements
P_{IN}	total electrical power to the pump
V_{LL}	input voltage, line-to-line
V_{LN}	output voltage, line-to-line
$\dot{v}$	volumetric flow rate
γ	ratio of specific heats
Δp	change in pressure
ρ	density
η	efficiency

TECHNICAL PUBLICATION

TESTING OF AN ANNULAR LINEAR INDUCTION PUMP FOR THE FISSION SURFACE POWER TECHNOLOGY DEMONSTRATION UNIT

1. INTRODUCTION

Fission surface power (FSP) systems could be used to provide power on the surface of the Moon, Mars, or other planets and moons of our solar system, as they are capable of providing excellent performance at any location, including those near the poles or other permanently shaded regions, and offer the capability to provide on-demand power at any time, even at long distances from the Sun. Fission-based systems also offer the potential for outposts, crew, and science instruments to operate in a power-rich environment while maintaining a relatively small footprint for the reactor system. NASA has been exploring technologies with the goal of reducing the cost and technical risk of employing FSP systems. A reference 40-kW$_e$ option has been devised that is cost competitive with alternatives while providing more power anywhere on the lunar surface for less mass. The reference FSP system is also readily extensible for use on Mars. On Mars, the system would be capable of operating through global dust storms and providing year-round power at any Martian latitude.

One key technology associated with the FSP system is the pump that circulates liquid-metal coolant through the reactor system. An annular linear induction pump (ALIP) was designed to support a quarter-scale, end-to-end technology demonstration unit (TDU) where 50 kW of simulated nuclear thermal power will be converted to 10 kW of electrical power. The ALIP was designed to support the TDU requirements and was tested in a stand-alone environment at representative reactor operating conditions. This Technical Publication (TP) details the performance testing of this prototypic TDU ALIP.

1.1 Fission Surface Power Technology Development

NASA and the Department of Energy are pursuing long-lead technology development for potentially supporting future integrated FSP systems. The major effort in the FSP technology project has been focused on a reference mission and concept. The reference mission is to provide electrical power to habitats on the lunar surface. The requirements derived from this mission are 40 kW$_e$ delivered to the habitat over a design lifetime of 8 years. Although many options exist, NASA's current reference FSP system uses a fast spectrum, pumped liquid sodium potassium- (NaK-) cooled reactor coupled to a Stirling power conversion subsystem. The reference system uses technology with significant terrestrial heritage that can perform at any location on the surface of the Moon or Mars. Detailed development of the FSP concept and the reference mission are documented in various other reports.[1–4]

The objectives of the FSP technology project are as follows:[5]

• Develop FSP concepts that meet expected surface power requirements at reasonable cost with added benefits over other options.

• Establish a nonnuclear hardware-based technical foundation for FSP design concepts to reduce overall development risk.

• Reduce the cost uncertainties for FSP and establish greater credibility for flight system cost estimates.

• Generate the key nonnuclear products to allow Agency decision makers to consider FSP as a viable option for potential future flight development.

The pump must be compatible with the liquid NaK coolant and have adequate performance to enable a viable flight system. Idaho National Laboratory (INL) was tasked with the design and fabrication of an ALIP suitable for the FSP reference mission. Under the program, a quarter-scale FSP technology demonstration is under construction to test the end-to-end conversion of simulated nuclear thermal power to usable electrical power intended to raise the entire FSP system to Technology Readiness Level 6. An ALIP for this TDU was fabricated under the direction of the INL and shipped to NASA Marshall Space Flight Center (MSFC) for testing at representative operating conditions. This pump was designed to meet the requirements of the TDU experiment. The ALIP test circuit (ATC) at MSFC, previously used to conduct performance evaluation on another ALIP[6] was used to test the present TDU pump for the FSP Technology Development program.

1.2 Nonnuclear Testing at Marshall Space Flight Center

The Early Flight Fission Test Facility was established by MSFC to provide a capability for performing hardware-directed activities to support multiple in-space nuclear reactor concepts by using a nonnuclear test methodology.[7,8] This includes fabrication and testing at both the module/component level and near prototypic reactor components and configurations, allowing for realistic thermal-hydraulic evaluations of systems. In the present testing, the ATC was slightly modified from the previous configuration[6] to provide more controllable heating of the NaK working fluid. The system and changes incorporated in this iteration are described in section 2, followed by measured performance results on the TDU ALIP.

2. ANNULAR LINEAR INDUCTION PUMP TEST CIRCUIT SETUP

The ATC apparatus, shown schematically in figure 1, was fabricated to allow for performance testing of liquid-metal induction pumps. The majority of the components of the test circuit are described in detail in "Performance Testing of a Prototypic Annular Linear Induction Pump for Fission Surface Power."[6] A brief overview of those unchanged components is provided in this section, with the balance of the section devoted to a discussion of the upgrades implemented for the testing described in this TP.
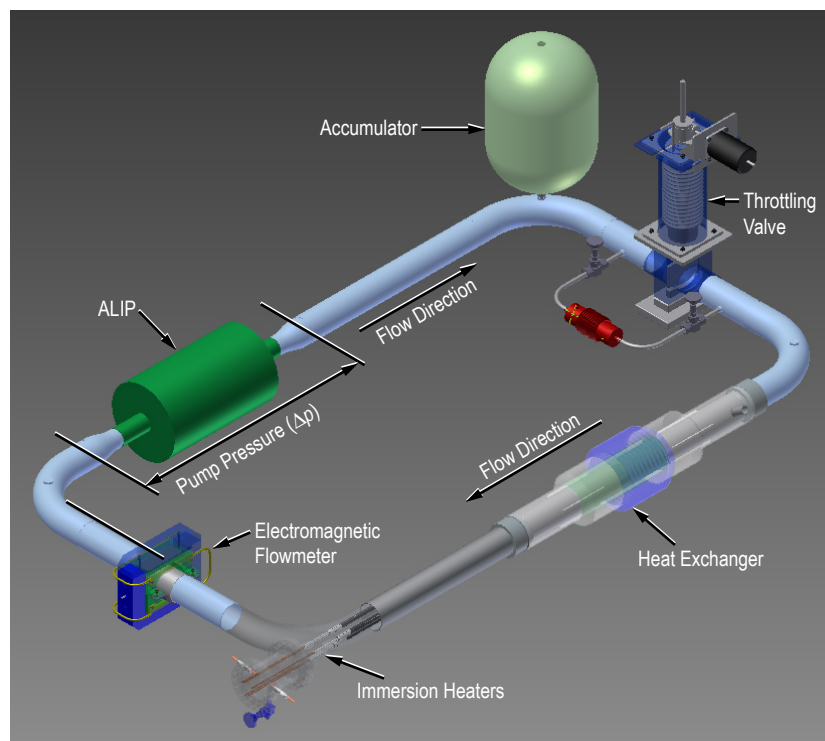
Figure 1. Schematic of the ALIP test circuit configured for TDU ALIP testing.

2.1 Overview of Components Unchanged From Previous Annular Linear Induction Pump Test Circuit Experiments

The test circuit consists of a large pipe (3-in, schedule 10, stainless steel (SS)) configured in a closed-loop shape with components positioned at different locations along the path. The large pipe size is employed to minimize the viscous pressure loss in the pipe, leaving the liquid NaK free to flow in the loop. Each of the components in the loop that are briefly mentioned in this subsection is described in greater detail in reference 6.

The throttling valve is included to provide an active control of the flow resistance in the loop. It is a gate valve that translates into and out of the flow, changing the flow impedance over a large range from minimal flow resistance to almost complete stagnation of the flow.

A gas-to-NaK counterflow concentric tube heat exchanger is employed to provide cooling and temperature control for the loop. The heat exchange medium is gaseous nitrogen with the heat exchanger sized to provide 10 kW of cooling.

The volumetric flow rate of NaK in the loop is measured using an electromagnetic flowmeter. It consists of two neodymium-iron-boron magnets opposing each other on opposite sides of the pipe, with magnetically permeable material forming the magnetic flux return. The flowmeter output is a voltage that arises from the motion of the conductive liquid metal across the magnetic field lines. That voltage is measured across the pipe and is proportional to the volumetric flow rate.

One of the two methods used to apply power to the pump was to employ an Allen Bradley PowerFlex 400 variable frequency drive (VFD), which permits testing up to 60 Hz. The VFD uses pulse-width modulation to produce a current waveform at the desired frequency that is approximately sinusoidal. Sine wave filtering of the three-phase waveform produces a voltage waveform that is also approximately sinusoidal, making it easier for the data acquisition (DAQ) system to measure the current, voltage, and power. When the VFD is used, the power to the pump is measured using an Ohio Semitronics two-meter wattmeter (model P-144D), which gives a voltage output proportional to the measured power, assuming the input current and voltage are sinusoidal waveforms.

Liquid NaK pressure measurements are obtained using metal diaphragm transducers manufactured by Delta Metrics. The transducers were water cooled to maintain them at a constant temperature, reducing thermal drift during the test. Independent pressure measurements were performed on the flow upstream and downstream of the ALIP, with the difference representing the pressure rise imposed on the fluid by the pump.

Temperature measurements on the flow loop are acquired using type K thermocouples. The thermocouples are inserted into small copper blocks, which are contoured on one side to match the curvature of the pipe. When the blocks are clamped to the pipe, they possess a large surface for thermal conduction. The clamp-on temperature measurement method has a fast response time, with changes in fluid temperature owing to a variation in operating conditions showing up almost immediately in the thermocouple data.

The DAQ and control system is based on National Instruments hardware and software. An in-house-developed LabVIEW™ application is used to control the experiment and acquire data from a PXI-1042 chassis, with an SCXI-1001 chassis used for signal conditioning.

2.2 Components in the System Changed for the Present Work

There were changes to the ATC that were implemented either to make it possible to test the TDU ALIP or as a result of lessons learned from previous ALIP testing.[6] These configuration changes are described in the remainder of this section.

2.2.1 Technology Demonstration Unit Annular Linear Induction Pump

The TDU ALIP consists of an annular duct surrounded by a series of electromagnetic coils. Three-phase power is supplied to the coils to generate an axially-traveling magnetic that induces currents in the electrically-conductive liquid NaK located within the duct. The induced currents interact with the externally-imposed magnetic field to generate net acceleration of the fluid in the streamwise direction. The flow rate and pressure developed by the pump are controlled by varying the voltage and frequency of the power supplied to the coils and by changing the overall NaK flow impedance in the loop. The pump was designed to operate nominally at 80 V and 40 Hz, producing NaK flow rates from 0.5 to 2.25 kg/s and developed pressures from 10 to 40 kPa. The peak operating temperature for the TDU and the FSP reactor systems is 800 K.

2.2.2 Immersion Heaters

In the present testing, a new immersion heating method was used to directly heat the liquid metal. Three graphite heaters previously designed and tested for use in other applications were placed in tubes directly in the flow. These heaters together are capable of delivering a theoretical maximum of >15 kW of thermal power (5 kW per heater) to the NaK. During operation of the ATC, about half of this power was required when heating to the maximum operating temperature of 525 ºC. The heating elements are cylindrical in shape, with a diameter of about 1.9 cm (0.75 in) and a length of about 58.4 cm (23 in). Figure 1 shows the location of the immersion heaters in the lower left-hand corner of the ATC. A study, summarized in appendix A, was performed to evaluate the pressure loss that would result when inserting heaters into the flow. In the study, the effect of inserting two, three, and four pins into the flow channel was evaluated. The amount of thermal energy available to be delivered to the NaK increased with the number of heaters, but the pressure drop in the loop also increased with the number of heaters. Based on the results of the study and the anticipated range of flow rates during a test, three heaters were selected for a balance of the ease of installation, adequate heat delivery, and acceptable pressure drop. Additionally, should one of the heaters fail, there would still be sufficient heating capacity available with the remaining two heaters.
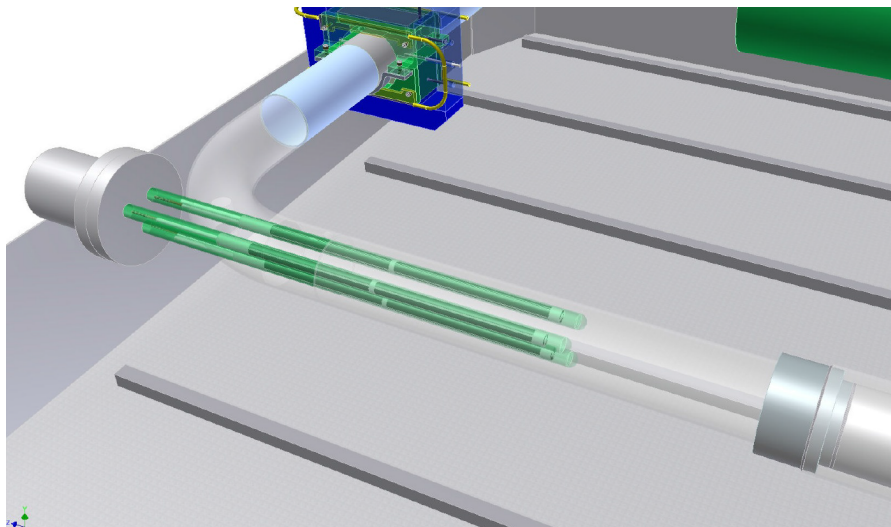

Figure 2. Three-dimensional view of elbow heater section.

The immersion heaters, presented in an enlarged view in figure 2 and in appendix B, consist of three metal-clad cylinders shown in green with each containing a resistive heating element and filled with helium (He). The He allows for sufficient thermal conduction between the graphite heaters and the inner diameter (ID) of the cylinders, permitting even heating of the cylinders and eliminating local hotspots. It is important to have even heating as a hotspot can potentially lead to a material failure and subsequent leakage of NaK into the immersion heaters. The heaters were wired in series to provide the correct resistance to permit the usage of the full current and voltage range of a 15 kW (150 V/100 A) Lambda power supply. Additionally, the heaters were designed so the heated sections were completely contained within the NaK flow and there was adequate room for thermal growth of the various components. All electrical connections were performed in the head section on the left side of figure 2. In the ATC, the performance of the immersion heater design was exemplary with extremely good transfer of heat to the NaK.

2.2.3 Variable Frequency Power Supply

A California Instruments model 9000LS/2-3-LAN-480-ADV programmable power supply was used to provide power to the ALIP. Table 1 lists the specifications of this two-chassis power supply unit.

Table 1. Two-chassis power supply unit specifications.

Input voltage (line-to-line)	480 V_{LL} ($\pm5\%$), three-phase
Input line current	2×12 A_{RMS} = 24 A_{RMS} @ 456 V_{LL}
Input line power	2×8.9 kVA = 17.8 kVA
Output voltage (line-to-neutral)	0–135 V_{LN} (low range) or 0–270 V_{LN} (high range), three-phase
Output power per phase at full-scale voltage	3 kVA
Maximum output current per phase at full power	29.6 A (low range)
Maximum output current per phase at full-scale voltage	22.2 A (low range)
Frequency range	45–1,000 Hz

All power supply setting and feedback data are communicated through an Ethernet interface. The AC power settings used included voltage, frequency, phase, and waveform type. The feedback measurements included the line-to-neutral DC and AC root mean square (RMS) components of the output voltage for each phase, the DC and AC RMS currents for each terminal including the neutral, the DC power, and the in-phase, apparent, and reactive components of the power for each output phase. Using this information, the power supply calculates and returns a power factor as part of the data.

The power supply can be programmed to regulate the output voltage using either internal or external sense lines. In the ATC, external sense lines were used, providing a measure of the voltage at the load. The output voltage range of the unit can be selected remotely, with the range of zero to 135 V_{LN} used in the present work. A slew rate can be specified for all programmed changes in the AC RMS voltage. The slew rate does not apply to changes in the DC voltage. Approximately instantaneous changes in the AC RMS voltage can be obtained by setting the slew rate to its maximum or

infinity. For ATC testing, a finite slew rate was used to prevent instantaneous changes in the voltage level, with the DC offset voltage always set to zero.

A slew rate also can be specified for changes in the frequency of the output waveform, with approximately instantaneous changes obtained by setting the slew rate to its maximum or infinity. For ATC testing, a finite slew rate was used to prevent instantaneous changes in the frequency.

The relative phase angle of each of the three output voltage phases can be programmed independently. The phase angle is programmed in degrees relative to an internal reference. Positive and negative phase angles are used to program leading and lagging phases, respectively. The phase angles were always set 120° apart in the present work. Direction of flow can be controlled by reversing two of the three output phases.

In addition to sinusoidal and square output waveforms, the power supply can be programmed to produce arbitrary user-defined waveforms. A user-defined waveform consists of 1,024 data points representing one full cycle of the waveform. The first data point specifies the relative amplitude at the zero-degree phase reference. The data points can be in any arbitrary units since the unit rescales the values to an internal format that removes any DC offset and ensures that the correct AC RMS output voltage is achieved.

Additional data can be obtained from the power supply. These include measurement of the percentage of total harmonic distortion and noise in each phase of the output voltage and current and the crest factor, which is defined as the ratio of the peak output current to the RMS output current.

3. PERFORMANCE TEST DATA

Three measurements must be simultaneously acquired to calculate the performance of any pump, including an ALIP. Those measurements are the volumetric flow rate ($\dot{v}$) and the pressure rise in the fluid (Δp) owing to the action of the pump and the total electrical power to the pump (P_{IN}). The efficiency is then defined as the net power into the fluid (equal to the volumetric flow rate multiplied by the pressure rise) over the total electrical power delivered to the pump:

$$\eta = \frac{\dot{v}\Delta p}{P_{IN}} \ . \tag{1}$$

Data were obtained at NaK temperatures of 125 °C, 325 °C, and the nominal FSP reactor operating temperature of 525 °C. Data are presented for the pump operating on VFD-supplied, three-phase power at 40 and 55 Hz, and on the variable frequency power supply (VFS) at 55 and 70 Hz. The pump was operated over a range of voltage levels from 30 to 120 V. Not all voltages and frequencies were tested for every condition.

Typically, data were acquired by first bringing the pump and loop temperature to a steady-state value. A constant pump voltage was set and the throttling valve was exercised through its entire range to obtain pump performance curves over a range of $\dot{v}$ and Δp values.

As in previous ALIP testing,[6] the data are remarkably clean, requiring no postprocessing before being plotted. In this section, the data are graphed as a series of scatter plots with each plot encompassing the entire data set for a given operating condition. Concentrations of data points represent flow conditions measured at steady-state flow conditions while the throttling valve was stationary (approximately 30–60 s dwell time). The individual dots forming the rest of the lines represent data obtained while the valve was transitioning from one setpoint to the next. Each efficiency point was computed using the flow rate, Δp, and input power as measured and recorded on the DAQ system. Testing with the VFD and the VFS were conducted on different days, with data corresponding to the same conditions (same temperature and a pump frequency of 55 Hz) plotted on the same graphs in this TP.

Pump performance data obtained at a NaK temperature of 125 °C are presented in figure 3. The average error bars for the pump performance data set presented in this TP are given in figures 3–5 to demonstrate the clean nature of the data. Data for pump operation at 325 and 525 °C are presented in figures 4 and 5, respectively. For completeness, the nominal design flow rate and Δp for the TDU are plotted as plus (+) symbols in figure 5(a), (c), and (e), showing that the TDU ALIP underperformed relative to the nominal design point.
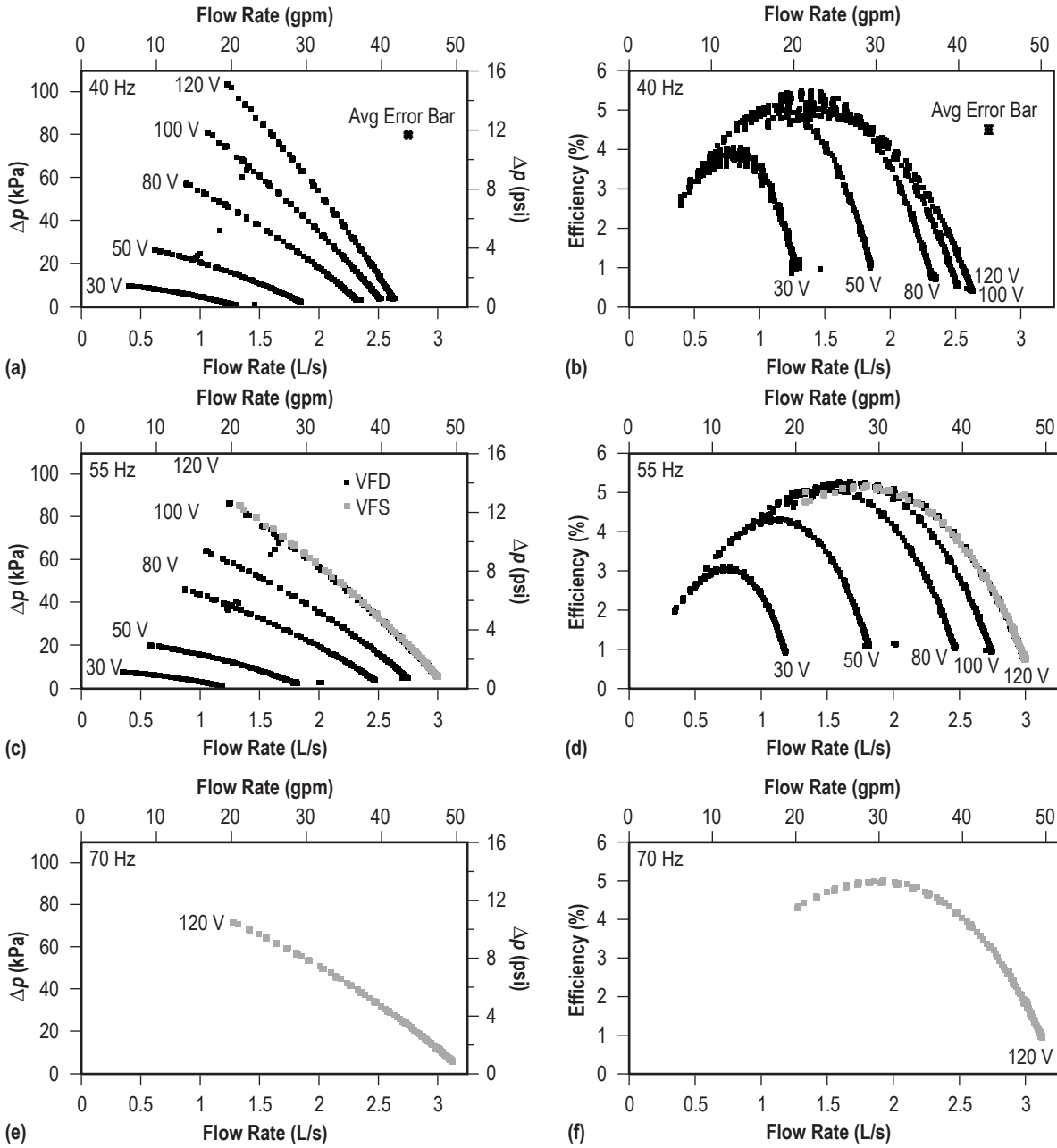
Figure 3. Raw data from operation at NaK temperatures of 125 ºC and pump frequencies of (a)and (b) 40 Hz, (c) and (d) 55 Hz, and (e) and (f) 70 Hz operating on either the VFD (black markers) or VFS (gray markers).

Figure 4. Raw data from operation at NaK temperatures of 325 ºC and pump frequencies of (a) and (b) 40 Hz, and (c) and (d) 55 Hz operating on the VFD.

Figure 5. Raw data from operation at NaK temperatures of 525 °C and pump frequencies of (a) and (b) 40 Hz, (c) and (d) 55 Hz, and (e) and (f) 70 Hz operating on either the VFD (black markers) or VFS (gray markers).
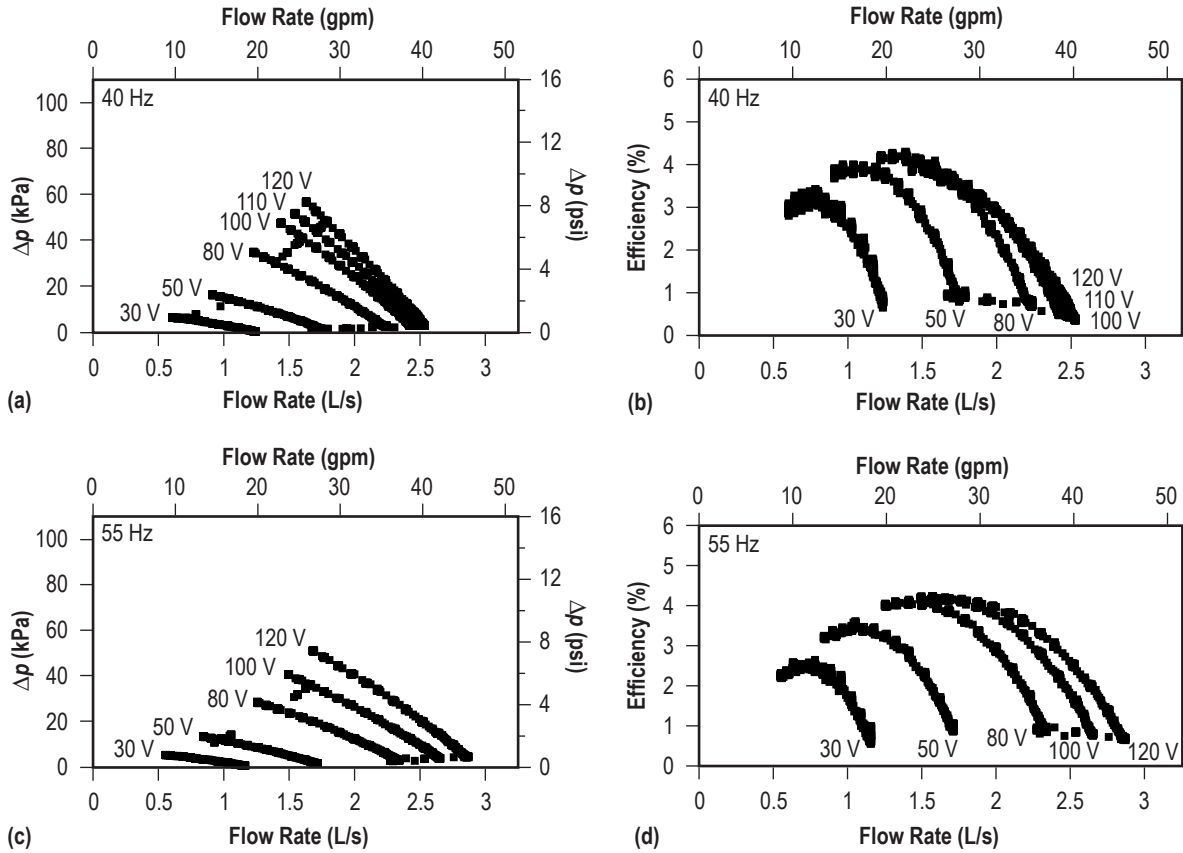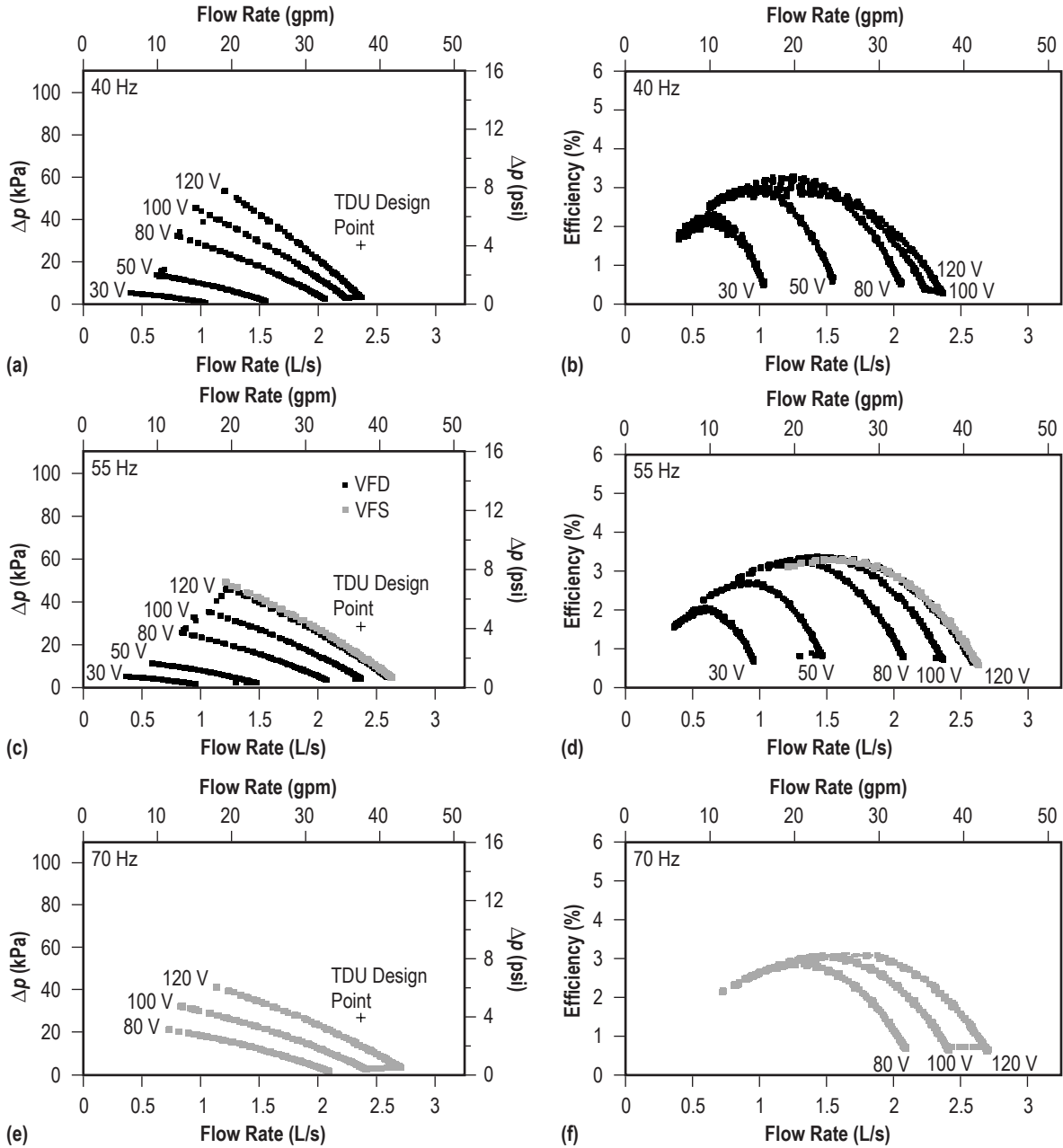
As was previously seen in ALIP testing,[6] the pump performance characteristics (achievable flow rate, Δp, and commensurate efficiency) all decrease as the temperature is increased. Changing the frequency has a large effect on the slope of the curves presenting Δp as a function of flow rate, but the frequency only appears to have a mild effect on the peak efficiency for a fixed temperature. The noticeable effect is the flow rate at which peak efficiency occurs, with the maximum occurring at higher flow rates as the frequency is increased. Data obtained using the VFD and the VFS operated at similar conditions (voltage, frequency) quantitatively agree and are relatively indistinguishable from each other.

11

To further investigate the effect of driving frequency on pump efficiency, the pump was operated at a constant voltage and the throttle valve was exercised through a number of cycles at different pump operating frequencies. The pump efficiency as a function of flow rate for each frequency is presented in figure 6. In the data set found in panel (a), the efficiency increases by small but finite amounts as the frequency is increased from 45 to 60 Hz. In panel (b), the efficiency begins to fall again above 60 Hz. However, in all cases, the change in peak efficiency does not greatly vary with frequency.
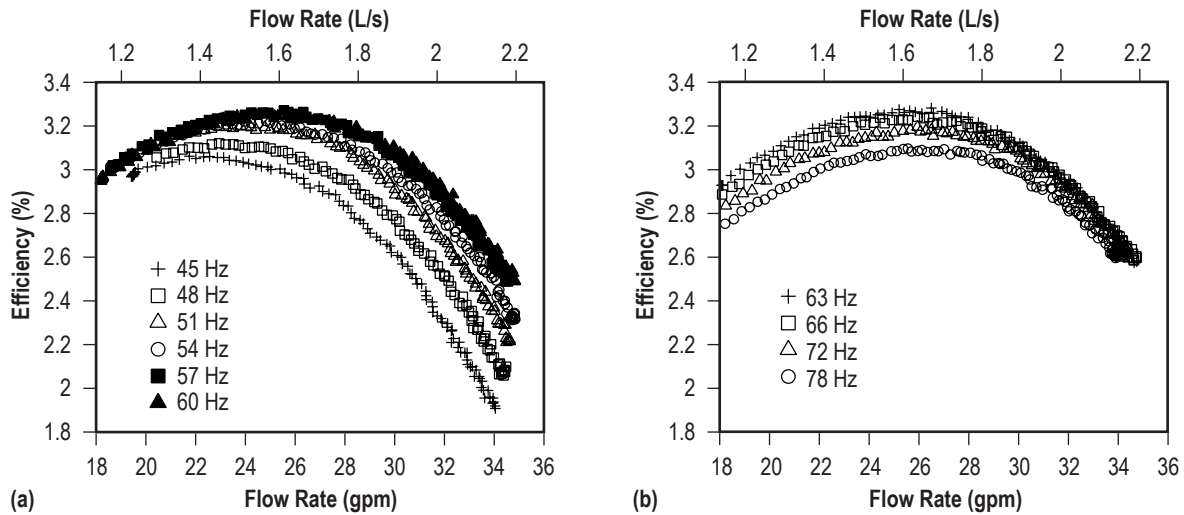

Figure 6. Raw efficiency data from sweeps of the throttling valve during operation at NaK temperatures of 525 °C for frequencies from (a) 45–60 Hz and (b) 63–78 Hz.

As with the FSP ALIP,[6] each phase of the TDU ALIP conducted a different current value for a fixed line-to-neutral voltage. This phenomenon is observed clearly in figure 7, where the phase currents are graphed as a function of time. The currents exhibit a stair-step behavior up and down as the throttling valve is opened and closed. Furthermore, the currents all exhibit changes as the voltage is changed. (While only one line-to-neutral RMS voltage is plotted, the data show that all three voltage waveforms are coincident.) The most important thing about the data is that they demonstrate that the current draw for each leg of the ALIP circuit is different by several amperes per phase.
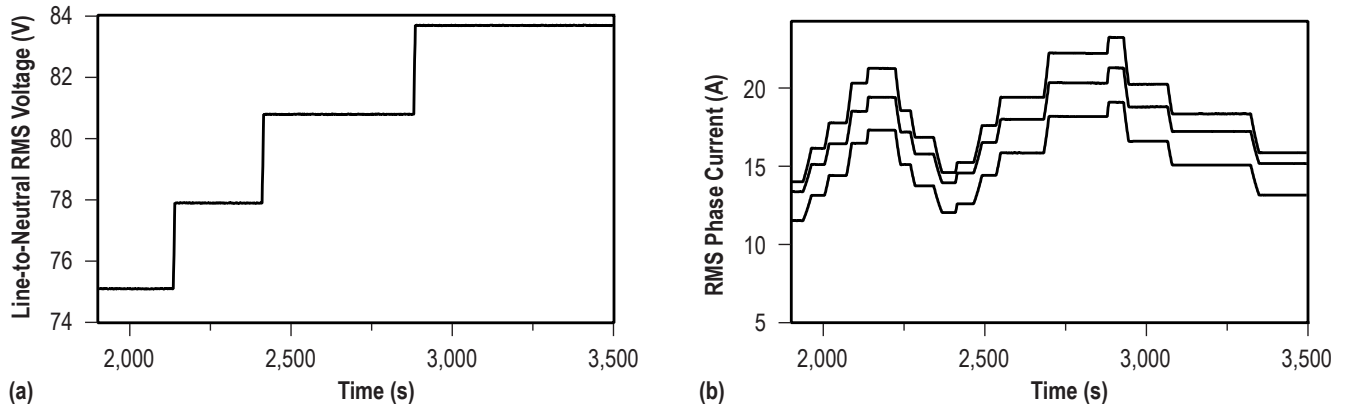
Figure 7. Data over several cycles of the throttling valve showing (a) applied line-to-neutral RMS voltages on all three input lines to the ALIP and (b) the resulting RMS currents for all three phases.

4. CONCLUSIONS

Testing was performed to quantify the performance of the TDU ALIP. The dedicated ATC apparatus was used for this purpose, with minor modifications to the configuration incorporated to improve the operational capabilities of the system. The results of the testing lead to the following conclusions:

- Relative to previous ATC operation, it was much easier to bring the system to temperature using the new immersion heater system. Furthermore, there were no adverse flow effects or abnormally high pressure drops noted over the entire operating envelope.

- The pump was tested at amplitudes of up to 120 V_{LN} input (line-to-neutral voltage) at NaK temperatures of 125 °C, 325 °C, and the nominal FSP reactor operating temperature of 525 °C.

- The pump was supplied with three-phase power from a VFD at frequencies of 40 and 55 Hz, and from a VFS at frequencies of 55 and 70 Hz. In addition, a scan of operation at different frequencies was performed using the VFS from 45 to 78 Hz.

- At the FSP reactor operating temperature of 525 °C, the performance spanned a range of flow rates from 0.3 to 2.75 L/s (4.8 to 43.6 gpm) and Δp levels from <1 to 55 kPa (<0.145 psi to roughly 8 psi). The maximum efficiency measured during this testing was approximately 3.5%.

- The efficiency of the pump decreased as the NaK temperature was increased.

- Measured performance at 55 Hz supplied by either the VFD or VFS when operating at comparable NaK temperatures exhibited quantitative agreement.

- The operating envelope at 525 °C fell short of the TDU design point at all frequencies.

- The pump exhibited some sensitivity to frequencies in terms of the flow rate at which the maximum efficiency occurred, but the maximum value of efficiency was relatively insensitive over the range of frequencies tested.

- For a constant line-to-neutral voltage on each phase of the pump, the phase currents differed from each other by several amps, indicating that the electrical loads presented by each phase of the pump were different.

APPENDIX A—IMMERSION HEATER PRESSURE DROP ANALYSIS

In the present work, resistive heating elements immersed in the liquid NaK were added to heat the fluid in the ATC. These heating elements are cylindrical in shape, with a diameter of about 1.9 cm (0.75 in) and a length of about 0.58 m (23 in). The elements are positioned within a large tube comprising the flow path for the ATC loop, which consists of SS tubing with an ID of 8.28 cm (3.26 in), and are aligned axially within the tubing as shown in figure 2 and appendix B.

The analysis detailed in this appendix was undertaken to provide a quantitative measure of the pressure drop the heater elements might introduce into the ATC. The Generalized Fluid System Simulation Program (GFSSP) computational code was used to estimate the heater-induced pressure loss within the ATC tubing. GFSSP is an MSFC-developed computational fluid network solver, and has been validated on many different fluid flow applications.[9]

A.1 Flow Model

The fluid properties of NaK[10] were introduced using the general fluid option available in GFSSP. The user supplies seven specific data files to GFSSP: thermal conductivity, density, viscosity, ratio of specific heats (γ), enthalpy, entropy, and the specific heat (C_p). The files provide these particular fluid properties as a function of temperature.

The flow path is constructed using a series of nodes and branches to analytically represent the flow path to be evaluated, in this case, the flow across a geometry representative of the immersion heater. The approach used in the present analysis was to model the geometry of the immersion heaters as a flow area reduction introduced by the heater elements that were represented by a square-edged reducer, where the reduced area is equal to the total cross-sectional area of the ATC tube minus the sum of the frontal area of the heater elements. The resulting equivalent diameter (D_{eqiv}) could then be determined from

$$D_{eqiv} = \sqrt{D_0^2 - nD_r^2} \ , \tag{2}$$

where D_0 is the ATC tube ID, D_r is the heater element diameter, and n is the number of heater elements.

The inside surface area plays a significant role in the generation of the pressure drop through the immersion heater, so it was necessary to determine an equivalent tube length, such that the equivalent length would provide the same surface area as that of the ATC tube inside wall and the immersion heater rods. The equivalent tube length (l_{eqiv}) that would provide the same total surface area is

$$l_{eqiv} = \frac{l\left(D_0 + nD_r\right)}{\sqrt{D_0^2 - nD_r^2}},$$

(3)

where l is the physical length of the immersion heater, i.e. 0.58 m (23 in).

Using these definitions, a GFSSP model was created using the computed equivalent diameters and lengths. The resulting GFSSP model, represented graphically, is shown in figure 8. The branch consisting of boundary nodes 5 and 6, and internal nodes 7–10 represents the immersion heater geometry. The contraction and expansion sections are represented by elements 78 and 910, with diameters given by equation (2). The length of element 89, located between the contraction and expansion, is found using equation (3). These equivalent diameters and lengths are summarized in table 2 for two, three, and four immersion heater elements.
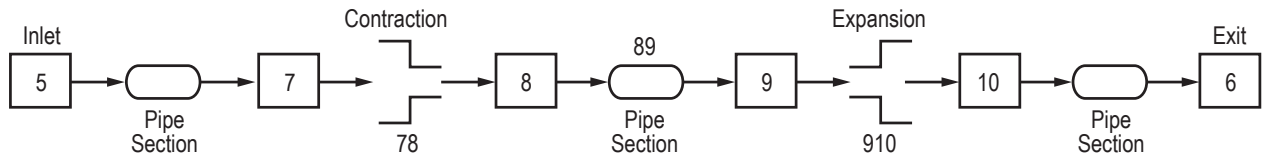

Figure 8. Immersion heater GFSSP model.

Table 2. Summary of equivalent diameters and lengths for various immersion heater geometries.

Number of Elements	2		3		4	
	cm	in	cm	in	cm	in
D_{eqiv}	7.82	3.08	7.60	2.99	7.34	2.89
l_{eqiv}	0.9022	35.52	1.076	42.38	1.263	49.74

A.2 Computational Results

The primary goal of this effort was to estimate the relative pressure losses induced by using two, three, and four elements in the immersion heater section of the ATC. With the geometry defined, the pressure losses were found by entering a range of supply pressures at the upstream boundary node (5) in the GFSSP model. Computed results for the two-, three-, and four-pin models are summarized in tables 3–5, respectively. The pressure values at nodes 5, 6, 7, and 10 are denoted, respectively, as P5, P6, P7, and P10.

16

Table 3. Results from two-element computations.

| P5 (kPa) | P6 (kPa) | P7 (kPa) | P10 (kPa) | Δp (Pa) | Flow Rate | | C_v |
					(kg/s)	(L/min)	[gpm/(psi)$^{1/2}$]
101.36	101.36	101.36	101.36	–	–	–	–
101.39	101.36	101.39	101.36	34.5	1.2	81.8	285.4
101.43	101.36	101.43	101.36	69.0	2.4	163.4	402.8
101.70	101.36	101.70	101.36	344.8	5.9	402.9	444.4
102.05	101.36	102.05	101.36	689.5	8.6	593.5	462.8
102.39	101.36	102.39	101.36	1,034.3	10.8	743.4	473.3
102.74	101.36	102.74	101.36	1,379.0	12.6	868.3	478.8
103.43	101.36	103.43	101.36	2,068.5	15.8	1087.0	489.4

Table 4. Results from three-element computations.

| P5 (kPa) | P6 (kPa) | P7 (kPa) | P10 (kPa) | Δp (Pa) | Flow Rate | | C_v |
					(kg/s)	(L/min)	[gpm/(psi)$^{1/2}$]
101.36	101.36	101.36	101.36	–	–	–	–
101.39	101.36	101.39	101.36	34.5	0.9	65.3	227.7
101.43	101.36	101.43	101.36	69.0	0.9	133.1	328.1
101.70	101.36	101.70	101.36	344.8	4.8	328.0	361.7
102.05	101.36	102.05	101.36	689.5	7.0	481.0	375.1
102.39	101.36	102.39	101.36	1,034.3	8.8	602.8	383.8
102.74	101.36	102.74	101.36	1,379.0	10.3	705.9	389.2
103.43	101.36	103.43	101.36	2,068.5	12.8	880.8	396.6

Table 5. Results from four-element computations.

| P5 (kPa) | P6 (kPa) | P7 (kPa) | P10 (kPa) | Δp (Pa) | Flow Rate | | C_v |
					(kg/s)	(L/min)	[gpm/(psi)$^{1/2}$]
101.36	101.36	101.36	101.36	–	–	–	–
101.39	101.36	101.39	101.36	34.5	0.8	54.0	188.4
101.43	101.36	101.43	101.36	69.0	1.7	115.9	285.8
101.70	101.36	101.70	101.36	344.8	4.1	284.2	313.5
102.05	101.36	102.05	101.36	689.5	6.0	415.4	323.9
102.39	101.36	102.39	101.36	1,034.3	7.5	518.5	330.1
102.74	101.36	102.74	101.36	1,379.0	8.8	609.1	335.9
103.43	101.36	103.43	101.36	2,068.5	11.0	759.0	341.7

The volumetric flow rates shown in tables 3–5 are converted from the computed mass flow rates given in the previous column using the density of NaK (871.5 kg/m^3 for this calculation). The flow coefficient (C_v) was found using the definition[11]

$$C_v = \frac{\dot{v}}{\sqrt{\Delta p \left(\dfrac{62.4}{\rho} \right)}} \, , \tag{4}$$

where $\dot{v}$ is the volumetric flow rate in gpm, Δp is the computed pressure drop in psi, located in the table, and ρ is the density of NaK in lbm/ft^3. The term 62.4/ρ yields the specific gravity of the fluid, with the resulting units on C_v being gpm/(psi)$^{1/2}$. The flow coefficient is generally given in imperial units and is a useful way of comparing the flow capacities of different valves and flow restrictions. The definition of C_v is the flow capacity in gpm of 60 °F water that a valve or restriction will pass for a pressure drop of 1 psi.

The pressure change (Δp) across the heater section for two, three, and four heater elements as a function of flow rate is presented in figure 9(a). Relative to the pressures expected based upon previous testing with the ATC,[6] the expected pressure drops for all three configurations are relatively small. The flow blockage and commensurate pressure drop is greater when there are more pins in the flow. However, for flow rates under 50 gpm, which is near the upper bound for flow rates in the ATC, it appears that the pressure drop will not exceed 138 Pa (0.02 psid).

The flow coefficient (C_v) across the heater section for two, three, and four heater elements as a function of flow rate are presented in figure 9(b). The higher the flow coefficient at a fixed flow rate, the more flow can be passed for a given pressure drop. As expected, the higher blockage caused by the larger number of pins results in a lower flow coefficient, especially at the higher flow rates.
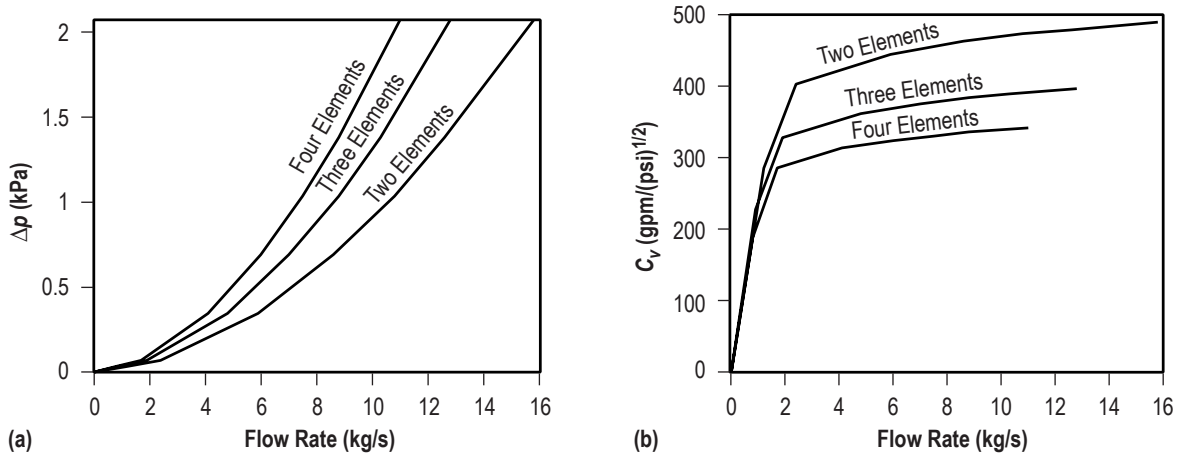
Figure 9. Across the heater section as a function of flow rate: (a) Pressure change
and (b) flow coefficient.

APPENDIX B—HEATER ELBOW ASSEMBLY

Figure 10 shows the heater elbow assembly drawing for the ATC.
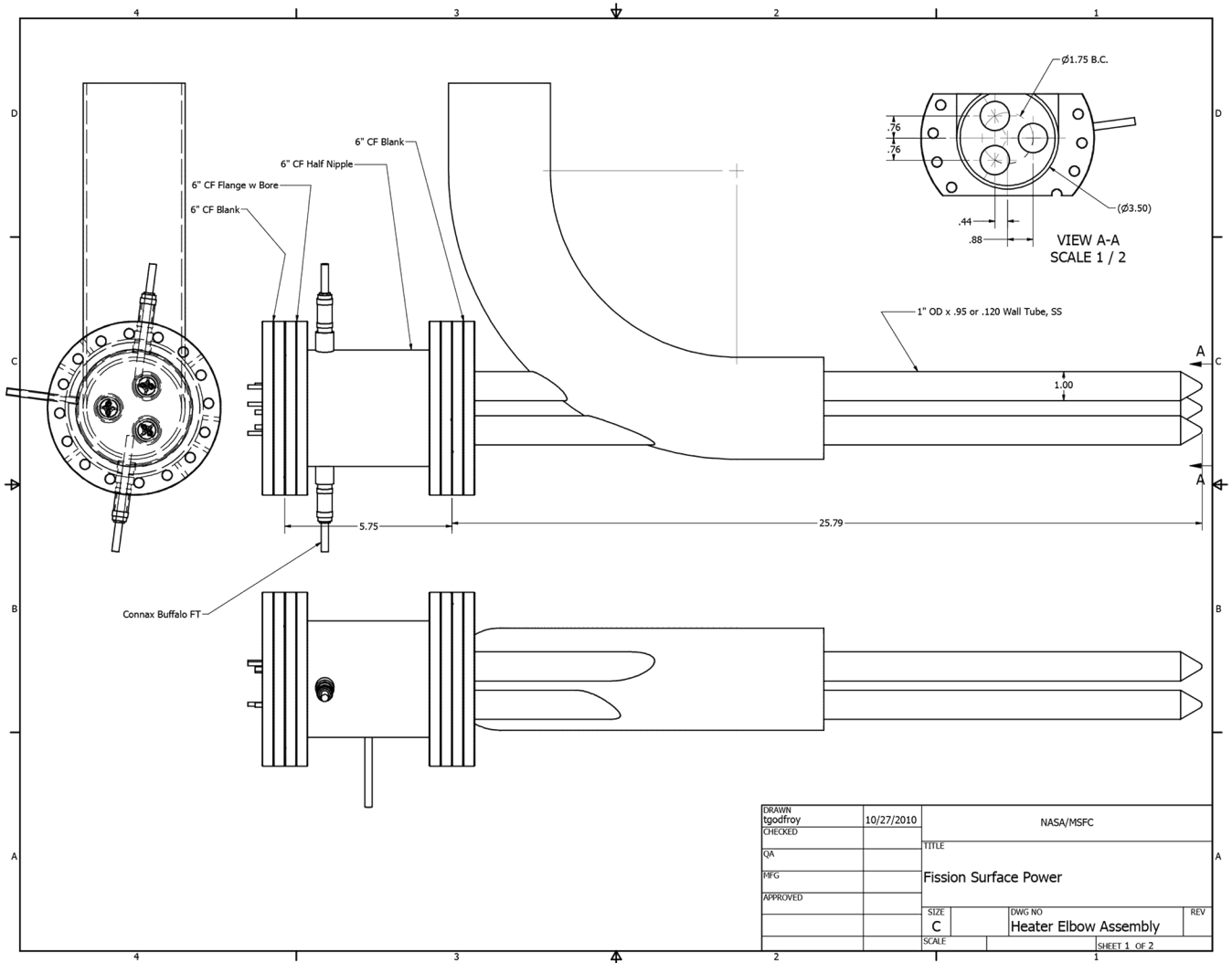

Figure 10. Heater elbow assembly drawing for the ATC.

REFERENCES

1. Nainiger, J.: "Affordable Fission Surface Power System Study Final Report," NASA Exploration Systems Mission Directorate Report, Glenn Research Center, Cleveland, OH, October 2007.

2. Mason, L.S.: "A Comparison of Fission Power System Options for Lunar and Mars Surface Applications," NASA/TM—2006–214120, Glenn Research Center, Cleveland, OH, February 2006.

3. Mason, L.S.: "A Practical Approach to Starting Fission Surface Power Development," NASA/TM—2006–214366, Glenn Research Center, Cleveland, OH, July 2006.

4. Mason, L.S.; Poston, D.; and Qualls, L.: "System Concepts for Affordable Fission Surface Power," NASA/TM—2008–215166, Glenn Research Center, Cleveland, OH, January 2008.

5. Palac, D.; Mason, L.; and Harlow, S.: "Fission Surface Power Technology Development Status," NASA/TM—2009–215602, Glenn Research Center, Cleveland, OH, March 2009.

6. Polzin, K.A.; Pearson, J.B.; Schoenfeld, M.P.; et al.: "Performance Testing of a Prototypic Annular Linear Induction Pump for Fission Surface Power," NASA/TP—2010–216430, Marshall Space Flight Center, Huntsville, AL, May 2010.

7. Godfroy, T.J.; Van Dyke, M.; and Dickens, R.: "Realistic Development and Testing of Fission Systems at a Non-Nuclear Testing Facility," *AIP Conf. Proc.*, Space Technologies and Applications International Forum, STAIF-2000, Vol. 504, pp. 1208–1210, 2000.

8. Van Dyke, M.; Godfroy, T.J.; Houts, M.; et al.: "Results of a First Generation Least Expensive Approach to Fission Module Tests: Non-Nuclear Testing of a Fission System," Space Technologies and Applications International Forum, STAIF-2000, *AIP Conf. Proc.*, Vol. 504, pp. 1211–1127, 2000.

9. Majumdar, A.; Steadman, T.; and Moore, R.: *GFSSP Users Manual*, Version 5.0, Marshall Space Flight Center, Huntsville, AL, February 2007.

10. Weatherford, Jr., D.W.: *The Properties of Inorganic Energy-Conversion and Heat-Transfer Fluids for Space Applications*, WADD-TR-61-96; Southwest Research Institute, San Antonio, TX, 1961.

11. Flow of Fluids through Valves, Fittings, and Pipe; Technical Paper No. 410, Crane Co., Stamford, CN, 1981.

REPORT DOCUMENTATION PAGE

Form Approved
OMB No. 0704-0188

1. REPORT DATE (DD-MM-YYYY) 01–08–2013	2. REPORT TYPE Technical Publication	3. DATES COVERED (From - To)

4. TITLE AND SUBTITLE	5a. CONTRACT NUMBER
Testing of an Annular Linear Induction Pump for the Fission Surface Power Technology Demonstration Unit	5b. GRANT NUMBER
	5c. PROGRAM ELEMENT NUMBER
6. AUTHOR(S)	5d. PROJECT NUMBER
K.A. Polzin, J.B. Pearson, K. Webster, T.J. Godfroy,* and J.A. Bossard**	5e. TASK NUMBER
	5f. WORK UNIT NUMBER

7. PERFORMING ORGANIZATION NAME(S) AND ADDRESS(ES) George C. Marshall Space Flight Center Huntsville, AL 35812	8. PERFORMING ORGANIZATION REPORT NUMBER M–1363

9. SPONSORING/MONITORING AGENCY NAME(S) AND ADDRESS(ES) National Aeronautics and Space Administration Washington, DC 20546–0001	10. SPONSORING/MONITOR'S ACRONYM(S) NASA
	11. SPONSORING/MONITORING REPORT NUMBER NASA/TP—2013–217487

12. DISTRIBUTION/AVAILABILITY STATEMENT
Unclassified-Unlimited
Subject Category 20
Availability: NASA CASI (443–757–5802)

13. SUPPLEMENTARY NOTES
Prepared by the Propulsion Systems Department, Engineering Directorate
*Maximum Technology Corporation, Huntsville, AL **BSRD, LLC/Yetispace, Inc., Huntsville, AL

14. ABSTRACT
Results of performance testing of an annular linear induction pump that has been designed for integration into a fission surface power technology demonstration unit are presented. The pump electromagnetically pushes liquid metal (NaK) through a specially-designed apparatus that permits quantification of pump performance over a range of operating conditions. Testing was conducted for frequencies of 40, 55, and 70 Hz, liquid metal temperatures of 125, 325, and 525 ºC, and input voltages from 30 to 120 V. Pump performance spanned a range of flow rates from roughly 0.3 to 3.1 L/s (4.8 to 49 gpm), and pressure heads of <1 to 104 kPa (<0.15 to 15 psi). The maximum efficiency measured during testing was 5.4%. At the technology demonstration unit operating temperature of 525 ºC the pump operated over a narrower envelope, with flow rates from 0.3 to 2.75 L/s (4.8 to 43.6 gpm), developed pressure heads from <1 to 55 kPa (<0.15 to 8 psi), and a maximum efficiency of 3.5%. The pump was supplied with three-phase power at 40 and 55 Hz using a variable-frequency motor drive, while power at 55 and 70 Hz was supplied using a variable-frequency power supply. Measured performance of the pump at 55 Hz using either supply exhibited good quantitative agreement. For a given temperature, the peak in efficiency occurred at different flow rates as the frequency was changed, but the maximum value of efficiency was relative insensitive within 0.3% over the frequency range tested, including a scan from 45 to 78 Hz.

15. SUBJECT TERMS
ALIP, annular linear induction pump, pump performance curve, space nuclear power, fission surface power, NaK

16. SECURITY CLASSIFICATION OF:			17. LIMITATION OF ABSTRACT	18. NUMBER OF PAGES	19a. NAME OF RESPONSIBLE PERSON STI Help Desk at email: help@sti.nasa.gov
a. REPORT U	b. ABSTRACT U	c. THIS PAGE U	UU	36	19b. TELEPHONE NUMBER (Include area code) STI Help Desk at: 443–757–5802

Standard Form 298 (Rev. 8-98)
Prescribed by ANSI Std. Z39-18